Preparation and Characterization of Nano-$CaCO_3$ Encapsulated with Polyacrylic and Its Application in PVC Toughness

Nongyue Wang,[1] Qingyan She,[1] Hongping Xu,[2] Yanmei Yao,[1] Liqun Zhang,[3] Xiongwei Qu,[1] Liucheng Zhang[1]

[1]*Institute of Polymer Science and Engineering, School of Chemical Engineering, Hebei University of Technology, Tianjin 300130, People's Republic of China*
[2]*Xiaoshan College, Zhejiang University of Radio and Television, Xiaoshan 311201, People's Republic of China*
[3]*Beijing University of Chemical Technology, Beijing 100029, People's Republic of China*

Received 11 November 2008; accepted 30 March 2009
DOI 10.1002/app.30508
Published online 7 October 2009 in Wiley InterScience (www.interscience.wiley.com).

ABSTRACT: The properties and morphology of nano-calcium carbonate (nano-$CaCO_3$) modified with the titanate coupling agent isopropyl trioleoyl titanate (IPTT) were characterized by Fourier transform infrared, thermogravimetric analyses, surface tension, and transmission electron microscopy. The results showed that the grafting ratio of IPTT on the surface of nano-$CaCO_3$ (IPTT-Ca) increased with IPTT content. IPTT-Ca/PBA/PMMA (IPTT-Ca/ACR, PBA/PMMA core-shell polymer, referred to ACR) latexes were prepared by seeded emulsion polymerization. They were then used to mix with PVC resin. The outer layer (PMMA) enhanced the dispensability of IPTT-Ca/ACR in the PVC matrix by increasing the interfacial interaction of these composite particles with PVC. The notched impact strengths of the blends were influenced by the weight ratio of IPTT-Ca to BA/MMA monomers, the weight ratio of BA/MMA. The relationships between the mechanical properties and the core-shell composite structures were elaborated. © 2009 Wiley Periodicals, Inc. J Appl Polym Sci 115: 1336–1346, 2010

Key words: fillers; emulsion polymerization; poly(vinyl chloride) blends; structure–property relations

INTRODUCTION

Strength and toughness are two important mechanical property indexes for polymers when they are used as constructed materials. At present, preparation of high-performance materials has attracted great interest of scientists. Poly(vinyl chloride) (PVC) has many merits, such as flame resistance, insulation, anti-abrasion, and stiffness. However, the notched impact strength of PVC is low when it is used as the constructed material.[1] Earlier, micrometric inorganic fillers were added into polymer matrixes to reduce costs, but the toughness of the composites tended to decrease significantly.[2,3] Elastic particles as fillers, such as ethylene-vinyl acetate copolymer,[4] chlorinated polyethylene,[5] methyl methacrylate–butadiene–styrene copolymer,[6] and polyacrylic rubber (ACR),[7,8] are the modification additives for PVC, but the enhancement of the toughness of the materials is at the cost of sacrificing the strength, stiffness, flowing property, and thermal resistance. Therefore the technology of rigid particle toughening has been reported by a number of scientific research groups.[9,10] This method requires the matrix possessing of certain ductility, and rigid particles can overcome the drawback of elastic toughening.

In recent years, the development of nanotechnology has brought the dawn of reinforcing and toughening polymers. Organic–inorganic nanocomposites have attracted great interest of many researchers because they have been deemed of an efficient strategy to upgrade properties of polymers that combine the advantages of polymer, such as elasticity, transparency, dielectric property, and moldability with those of inorganic nanoparticles. Therefore, their

Correspondence to: X. Qu (xwqu@hebut.edu.cn).
Contract grant sponsor: Key Project of Natural Science Foundation of Hebei Province; contract grant number: E2007000077.
Contract grant sponsor: Research foundation from Key Lab for Nanomaterials, Ministry of Education; contract grant number: 2007-2.
Contract grant sponsor: Excellent Project of Ministry of Personal Resources of China; contract grant number: 2006-164.
Contract grant sponsor: Start-up Foundation from Ministry of Education of China; contract grant number: 2007-24.
Contract grant sponsor: Research foundation from Key Lab of Beijing City on Preparation and Processing of Novel Polymer Materials; contract grant number: 2006-1.
Contract grant sponsor: Distinguished Youth Scientist of NSF; contract grant number: 50725310.

applications are enlarged from mechanics and tribology to optics, magnetism, and electronics.[11,12] However, it is very difficult for inorganic nanoparticles to disperse uniformly in the polymer matrixes at the nanometer scale because they have very high surface energy and are prone to agglomerate into large particles during the preparation of the composites. Many approaches have been tried to solve these problems, for example, the vapor deposition technique, nanoreactor, intercalation polymerization, and supermolecular self-assembly technique. Among these methods, in situ polymerization is the most desirable for preparing nanocomposites because the types of inorganic nanoparticles and monomers can vary widely to meet the various requirements.[13–15] Wang and coworkers[16,17] used ultrasonic technology to prepare polymer/inorganic nanocomposites and studied the main effects systematically on ultrasonic-induced encapsulating emulsion polymerization. Xu et al.[18] obtained nanosilica/thermoset polymer composites through ultraviolet curing technology and investigated the thermostability and mechanical properties of nanocomposites. Other researchers had successfully synthesized nano-silica/polymers using silicas with different sizes through emulsion polymerization.[19–22]

From the previous literature, researches of nano inorganic/organic composites focused on the silica, alumina,[23] titanium dioxide,[24,25] and montmorillonite,[26–28] whereas the studies of nano-calcium carbonate (nano-$CaCO_3$) were very few, to our knowledge. $CaCO_3$ is a kind of low-cost inorganic material that can be obtained easily. In this article, we characterize the changes on the $CaCO_3$ surface properties modified with a coupling reagent, isopropyl trioleoyl titanate (IPTT), by thermogravimetric analysis (TGA), Fourier transform infrared (FTIR) spectroscopy, surface tension, and transmission electron microscopy (TEM). IPTT-$CaCO_3$/PBA/PMMA (IPTT-Ca/ACR) composite latexes are synthesized successfully through seeded emulsion polymerization. The mechanical properties of IPTT-Ca/ACR and PVC blends are also investigated.

EXPERIMENTAL

Materials

Nano-$CaCO_3$ with the mean particle diameter of 25 $\pm$ 5 nm was treated with stearic acid from Mengxi Group Company, Mengxi City, China. before use, the particles were dried in an oven at 110°C under vacuum for 4 h to eliminate the physically absorbed and weakly chemisorbed species. The coupling agent IPTT (supplied by Nanjing Shuguang Chemical Reagent, Nanjing City, China), toluene, and ethanol (AP; purchased from Tianjin Chemical Reagent, Tianjin City, China) were used as received. *n*-Butyl acrylate (BA) was washed three times with 2% sodium hydroxide solution and deionized water, dried over $CaCl_2$ overnight, and then distilled. Methyl methacrylate (MMA), CP, from Tianjin Chemical Reagent Company, was distilled under reduced pressure. 1,4-Butanediol diacrylate (BDDA) and allyl methacrylate (ALMA), CP, were purchased from Tianjin Tianjiao Chemical, Tianjin City, China. Sodium dodecylsulfate (SDS), AP, from Tianjin Kermel Chemical Reagents Development Centre, Tianjin City, China, and potassium persulfate ($K_2S_2O_8$, KPS), AP, from Tianjin University Chemical Reagent Company, Tianjin City, China, were used without purification. PVC resin (SKL-1000), commercial product, was purchased from Tianjin Dagu Chemical, Tianjin City, China. Organotin, commercial product, was purchased from Beijing No. 2 Chemical Company, Tianjin City, China. Calcium stearate and stearyl alcohol, CP, was supplied from Tianjin Chemical Reagent Company, Tianjin City, China. They were used as received. Deionized water was used for all polymerization and treatment processes.

Surface Treatment of nano-$CaCO_3$ particles

Grafting reaction was carried out in toluene (120 mL) at different reaction temperatures under N_2 atmosphere. Dried nano-$CaCO_3$ (4 g) was suspended in toluene under mechanical stirring and ultrasonic dispersing. The weighed IPTT was dissolved in ethanol (10 mL) and mixed with nano-$CaCO_3$ in a flask. The product was heated and reacted for specified times, cooled to room temperature, and then separated by TDL-40B centrifugal machine. After drying at 70°C for 18 h under vacuum, the mixture was extracted using Soxhlet extractor for 18 h with toluene. The residual product was finally dried at 70°C under vacuum condition for 24 h.

Preparation of IPTT-Ca/ACR core-shell composite latexes

Nano-$CaCO_3$ particles modified with IPTT (IPTT-Ca) were emulsified in water containing the emulsifier, SDS, by the mechanical stirring and ultrasonic dispersing, and adjusting the pH value from 8 to 10 with sodium hydroxide solution. The amounts of the components are listed in Table I. After the seeded preemulsion was introduced into the reaction vessel and heated to 75°C, it was deoxygenated by bubbling with high pure nitrogen for 20 min. Initiator (KPS) solution, monomer (BA), cross-linking agent (BDDA), and grafting agent (ALMA) were dropped into the seeded latex at a rate of about 10 droplets per minute. After emulsion polymerization was carried out for 40 min, a small amount additional

TABLE I
Recipe of Synthetic IPTT-Ca/ACR Composite Latex

	Component	Mass (g)
Seed stage	IPTT-Ca	9.5
	SDS	0.45
	H_2O	210
Growth stage		
Core layer	BA	30
	BDDA	0.20
	ALMA	0.10
	KPS/H_2O	0.30/15
	SDS/H_2O	0.40/20
Shell layer	MMA	20
	KPS/H_2O	0.10/15
	SDS/H_2O	0.20/20

emulsifier (SDS) was added each hour. When the monomers were dropped completely, the core growth-stage of polymerization was maintained for 1 h at 75°C. Introducing the residual initiator, the latex started to drop MMA monomer at a rate of about six droplets per minute. The system was maintained at 75°C for 1.5 h after the monomer was dropped completely. The composite latex was refrigerated to coagulate and demulsify, and the precipitated materials were then filtered, washed, and dried under vacuum at 45°C for 12 h to get IPTT-Ca/PBA/PMMA (IPTT-Ca/ACR) composite particles.

Preparation of blending samples with IPTT-Ca/ACR particles and PVC resin

The synthesized IPTT-Ca/ACR particles were mixed with PVC resin and other determined quantity additives. The processing recipe was 100 parts of PVC resin, 2.5 parts of organotin, 0.8 part of calcium stearate, 0.8 part of stearyl alcohol, and 8 parts of IPTT-Ca/ACR. All components were first premixed in a high-speed mixer and then processed on a laboratory two-roll mill between 170 and 175°C for 7 min. Two- or 4-mm-thick plates were pressed at the temperature of 178–182°C. The plates were cooled under a cooling press.

Characterization

Contact angle measurement

Considerable attention had been paid to a utility method of measuring the surface free energy of a solid in recent years, for example, the measurement of contact angles.[29,30] Nano-$CaCO_3$ particle is a kind of inorganic material that has high surface energy and surface tension. Therefore, the single-liquid method is difficult to measure its contact angle with water only. The double-liquid method is used to investigate surface properties of nano-$CaCO_3$ in this article. The solid samples are immersed in hydrocarbon saturated with water, and the water saturated with hydrocarbon is then injected on the solid sample and the contact angle of the second liquid on the surface of the sample is measured. Nano-$CaCO_3$ particles were pressed into sheets using a hydraulic pressure machine. The saturated solutions of hexane and *n*-octane in water were prepared, and the saturated solutions of water in hexane and *n*-octane were obtained simultaneously. The contact angle on the surface of nano-$CaCO_3$ was measured using the JY-82 contact angle instrument with solution I (the saturated solution of water in hydrocarbon) as immersed liquids and solution II (the saturated solution of hydrocarbon in water) as tested liquids. Three measurements were carried out for each date, and the error was effective in the range of 2°.

Calculation of surface tensions of nano-$CaCO_3$ and IPTT-Ca particles

The modified Fowkes theory was deduced by Tamai et al.,[31] which could be expressed in the following equation:

$$r_H - 2\left(r_S^d r_H\right)^{1/2} = r_W - 2\left(r_S^d r_W^d\right)^{1/2} - I_{SW} + r_{HW}\cos\theta \quad (1)$$

$$I_{SW} = 2\left(r_S^p r_W^p\right)^{1/2} \quad (2)$$

where r_H is the surface tension of hydrocarbon, r_S^d, its dispersion component of the surface tension of the solid sample, r_S^p, its polarity component of the surface tension of the solid sample, r_W, the surface tension of water, r_W^d, water's dispersion component of r_W, r_W^p, water's polarity component of r_W, r_{HW}, the interface tension on the surface between paraffin and water, θ, the contact angle measured. The values of r_H, r_W, r_W^d, and r_{HW} could be obtained from the references.[32,33] The values of r_S^d and I_{SW} can be calculated from eq. (1) through measuring the contact angles of different saturated hydrocarbons. The value of r_S^p can be obtained from the eq. (2). Finally, the value of the surface tension (r_S) of the nano-$CaCO_3$ can be obtained through eq. (3).

$$r_S = r_S^d + r_S^p \quad (3)$$

Determination of grafting ratio (R_g)

The treated nano-$CaCO_3$ particles were Soxhlet-extracted with toluene. The grafting ratio of the titanate coupling agent (IPTT) on the surface of nano-$CaCO_3$ was measured using a TGA (Dupont STD-2960) at a scanning rate of 10°C/min under nitrogen atmosphere. The grafting ratio (R_g) was calculated by eq. (4):

$$R_g = \left(\frac{W_1'}{W_1} - A - \frac{W_0'}{W_0}\right) \times 100\% \quad (4)$$

where W_1 is the starting weight of the IPTT-Ca particles, W_1' is the residual weight of the IPTT-Ca particles at 600°C; A is a fraction content of TiO_2 contained in the form of the grafted IPTT coupling agent on the surface of nano-$CaCO_3$ particles, while the hydrocarbon radicals were completely degraded at the designed temperature; W_0 is the starting weight of untreated nano-$CaCO_3$ particles, and W_0' is the residual weight of untreated nano-$CaCO_3$ particles at 600°C.

Measurement of the latex particle diameter and its distribution

The latex particle diameters and their distribution were measured with the aid of dynamic light scattering analyzer by Malvern Instrument, Zetasizer HS3000.

TEM observation

Treated and untreated nano-$CaCO_3$ particles were suspended in ethanol by mechanical stirring and ultrasonic dispersing, whereas the IPTT-Ca/ACR composite latex was suspended in water. A drop of diluted dispersion was put on a carbon film supported by copper and placed in the HITACHI H-800 TEM. The IPTT-Ca/ACR particles dispersed in PVC matrix were determined by TEM. The samples were directly observed without dyeing.

Mechanical properties of IPTT-Ca/ACR particles and PVC blends

The Charpy notched impact tests on the specimens were carried out with a pendulum-type impact tester (CXJ-40, Chengde Testing Instruments, Chengde, China) at temperatures of 23°C and −20°C. At least five runs were made so we could report the average. The tensile properties were measured on an Instron (model 1122) tensile machine (Buckinghamshire, UK) according to ASTM D 638 with a crosshead speed of 20 mm/min at room temperature.

Scanning electron microscopy measurement

A Philips XL30 Scanning electron microscope (SEM) was used to study and record the fractured surfaces of the mixing samples. The fractured specimen surfaces were coated with a thin layer of gold. The coating was carried out by placing the specimen in a high vacuum evaporator and vaporizing the metal held in a heated tungsten basket.

RESULTS AND DISCUSSION

Surface treatment of nano-$CaCO_3$ particles

Calcium carbonate has been extensively used as a particulate filler in the manufacture of paint, paper, rubber, plastics, and so on. It is often treated with a surface modifier to enhance its incorporation and dispersion in the matrix and to improve mechanical properties of the composites. The CO_3^{2-} on the surface of calcium carbonate is absorbed by the moisture in the atmosphere, as described in eq. (5). A number of hydroxyl groups are generated on the surface of calcium carbonate particles due to hydrolyzation, which is described as the following chemical equation.[34] Therefore, the titanate coupling agent can be grafted onto the surface of calcium carbonate through the chemical reaction between hydroxyl of calcium carbonate and alkoxyl of titanate, as shown in eq. (6).

$$Ca^{2+}\,|\,CO_3^{2-} + H_2O \rightarrow Ca^{2+}(OH^-)_2 + CO_2\uparrow \qquad (5)$$

$$(CaCO_3) - OH + RO - Ti - (OX - R' - Y)_3 \rightarrow (CaCO_3) - O - Ti - (OX - R' - Y)_3 + ROH \qquad (6)$$

The values of surface tension of nano-$CaCO_3$ treated under different contents of the titanate coupling agent are listed in Table II. From Table II, we observed that the contact angle of the solution I drop (the saturated water in the paraffin) on the nano-$CaCO_3$ sheet surface that was immersed in the solution II (the saturated hydrocarbon with water) increased with the addition of the titanate coupling agent. It indicated that the hydrophilicity of nano-$CaCO_3$ became weaker after being treated by the titanate coupling agent. The surface tension of nano-$CaCO_3$, which was calculated from the modified Fowkes equations, decreased gradually with increasing content of the titanate coupling agent. The grafting ratio can be calculated from the results of Figure 1, corresponding to different contents of the titanate coupling agent. The result is listed in Table II also. The grafting ratio increased quickly when the IPTT content was less than 9 wt %. Above that, the change of grafting ratio became slow. Thus, the 5 wt % IPTT content modified on the calcium carbonate surface was used, and this modification resulted in the following semicontinuous emulsion polymerization of the IPTT-Ca/ACR composite latex.

Figure 2 illustrates the FTIR absorption spectra of the treated nano-$CaCO_3$ particles with different weight ratios of IPTT to $CaCO_3$. The IR absorption bands at 1433, 871, and 712 cm^{-1} were attributed to Ca—O stretching and bending vibrations, respectively.[35] The characteristic band at 1720 cm^{-1} was relative to C=O symmetric stretching absorption bands of IPTT. The peaks at 2926 and 2850 cm^{-1}

TABLE II
Contact Angle, Surface Tension, and Grafting Ratio on the Surface of $CaCO_3$ Treated with IPTT at Different Treatment Conditions

Reaction Condition	Contact Angle (°)		Surface Tension ($\times 10^3$ N/m)	Grafting Ratio (wt %)
	Hexane Solution	*n*-Octane Solution		
IPTT/$CaCO_3$ (wt %)[a]				
0	146.0	133.7	181.2	0
3	157.0	144.3	129.6	1.84
5	165.2	152.3	91.4	2.70
9	171.0	156.3	79.0	3.58
11	173.0	175.7	73.5	3.74
Reaction temperature (°C)[b]				
30	153.0	140.0	156.7	0.81
45	156.7	144.0	131.2	1.84
60	159.7	148.0	102.5	2.31
75	165.2	152.3	91.4	2.70
90	169.3	155.0	84.3	3.04
100	169.3	154.7	87.0	2.83
Reaction time (min)[c]				
0	146.0	133.7	181.2	0
10	154.0	141.3	145.7	0.88
30	158.6	146.6	111.5	2.03
50	165.2	152.3	91.4	2.70
70	166.7	153.3	88.8	2.86

[a] Reaction time: 50 min; reaction temperature: 75°C.
[b] Reaction time: 50 min; weight ratio of IPTT to nano-$CaCO_3$: 5%.
[c] Reaction temperature: 75°C; weight ratio of IPTT to nano-$CaCO_3$: 5%.

were assigned to H—C—H asymmetric and symmetric stretching vibrations, respectively.[36] As the samples were extracted by Soxhlet extraction with toluene, the physically absorbed IPTT had been removed. The FTIR absorption spectra of the extracted IPTT/nano-$CaCO_3$ samples could be tentatively ascribed to chemical bonding, i.e., the amount of the grafted IPTT on the surface of nano-$CaCO_3$ increased with the increase of the IPTT content in the treatment systems.

The morphologies of untreated and treated nano-$CaCO_3$ are characterized by TEM, as shown in Figure 3. We observe that the untreated nano-$CaCO_3$ exhibited a large number of agglomerates in Figure 3(a), whereas the loosed structures of IPTT modified nano-$CaCO_3$ particles are observed in Figure 3(b). After nano-$CaCO_3$ particles were modified with IPTT, the hydrophobization gradually raised and its hydrophilicity weakened on the surface of nano-$CaCO_3$, and the surface energy was also reduced so

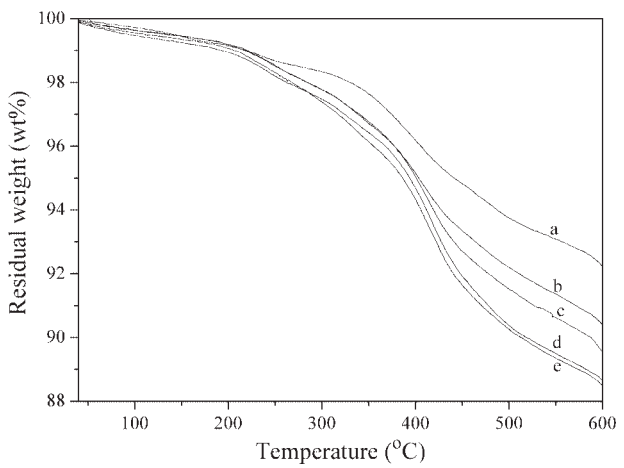

Figure 1 TGA curves of residual weight percent of the treated nano-$CaCO_3$ with different weight ratios of IPTT to nano-$CaCO_3$: (a) 0%, (b) 3%, (c) 5%, (d) 9%, and (e) 11%.

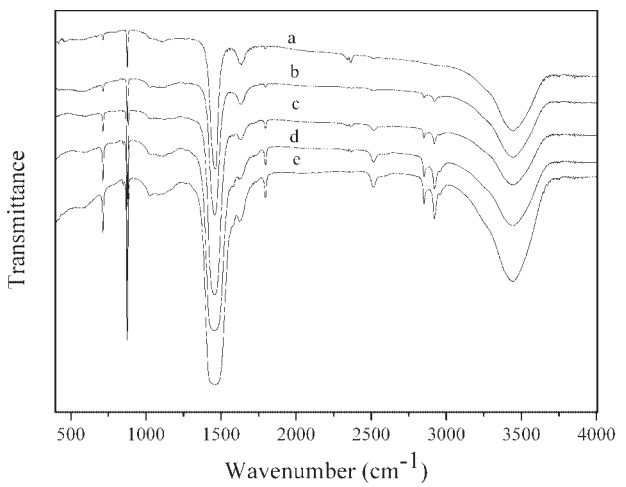

Figure 2 FTIR spectra of nano-$CaCO_3$ treated with different weight ratios of IPTT to nano-$CaCO_3$, (a) 0%, (b) 3%, (c) 5%, (d) 9%, and (e) 11%.

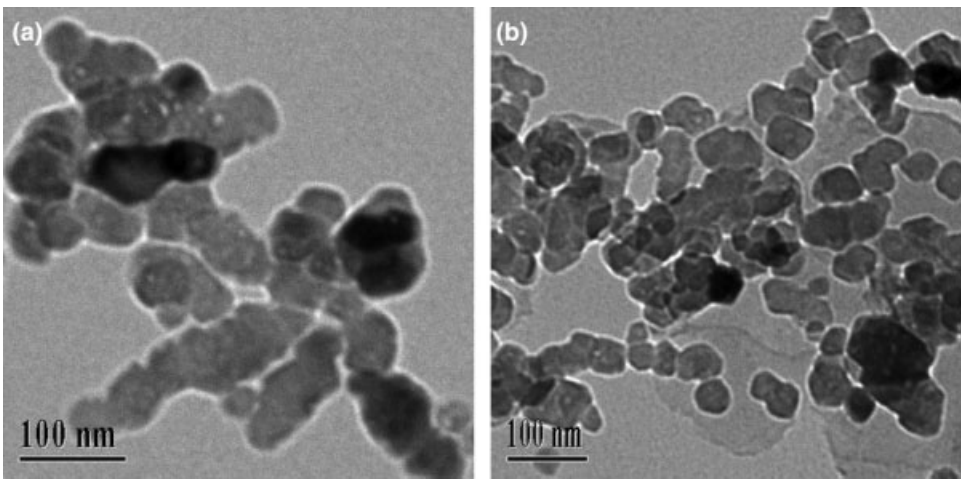

Figure 3 TEM images of calcium carbonate dispersed in ethanol (a) nano-$CaCO_3$ untreated and (b) nano-$CaCO_3$ treated by IPTT.

as to weaken the trend of agglomeration. The grafting ratio IPTT coupling agent on the surface of nano-$CaCO_3$ particles was 2.70 wt %. FTIR spectra, TGA curves, surface tension calculation, and TEM observation showed that IPTT molecules had been effectively grafted onto the surface of nano-$CaCO_3$ particles.

Table II also lists the surface parameters of nano-$CaCO_3$ obtained with 5 wt % of titanate coupling agent at different reaction temperatures. The surface tension of nano-$CaCO_3$ decreased significantly with the increase of the reaction temperature. With the increase of the reaction temperature, the functional groups were activated, and condensation reaction occurred between isopropyl groups of IPTT and hydroxyl groups on the surface of the nano-$CaCO_3$ particles.[34] When the reaction temperature increased to 90°C, the value of contact angle reached the smallest, and the grafting ratio on the surface of nano-$CaCO_3$ increased to 3.04 wt %. After the reaction temperature was above 90°C, the grafting ratio decreased slightly. The data of the surface tension are consistent with the grafting ratio on the surface of nano-$CaCO_3$ calculated from TGA curves, as shown in Figure 4.

The effects of the reaction time on the surface properties of nano-$CaCO_3$ particles are listed in Table II also. The surface tension decreased rapidly when the reaction time was over 50 min. After that, the tendency of decrease changed slowly. From TGA data in Figure 5, we can obtain the same results about the effect of reaction time on the grafting ratio. Therefore, the suitable treatment conditions of nano-$CaCO_3$ with IPTT coupling agent were: reaction temperature 75°C, reaction time 50 min, weight ratio of IPTT to nano-$CaCO_3$ 5% used in the following discussion, and the grafting ratio was 2.70 wt %.

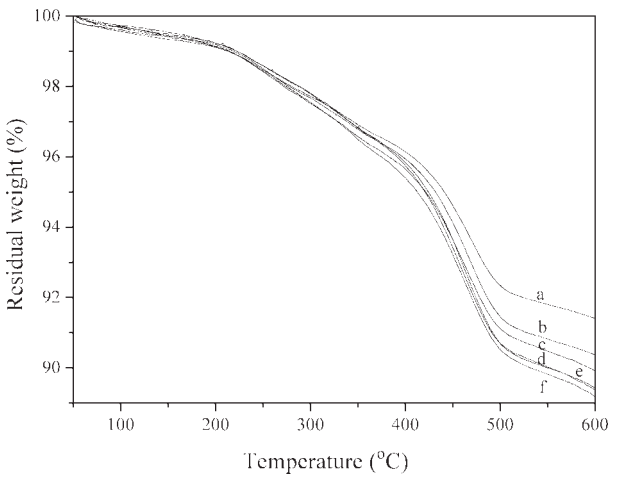

Figure 4 TGA curves of residual weight percent of the treated nano-$CaCO_3$ at different treated temperatures: (a) 30°C, (b) 45°C, (c) 60°C, (d) 75°C, (e) 90°C, and (f) 100°C.

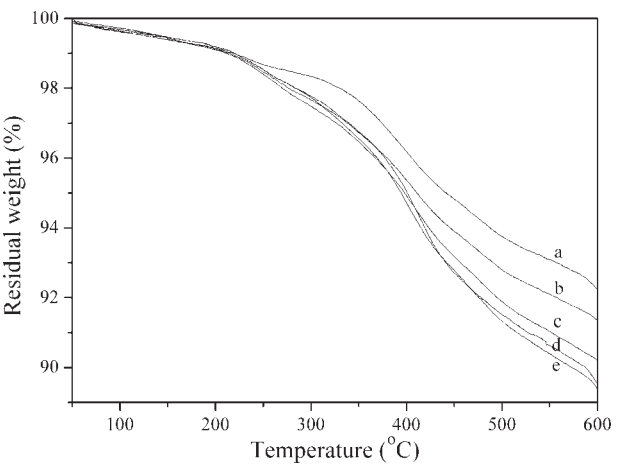

Figure 5 TGA curves of residual weight percent of the treated nano-$CaCO_3$ at different treated times: (a) 0 min, (b) 10 min, (c) 30 min, (d) 50 min, (e) and 70 min.

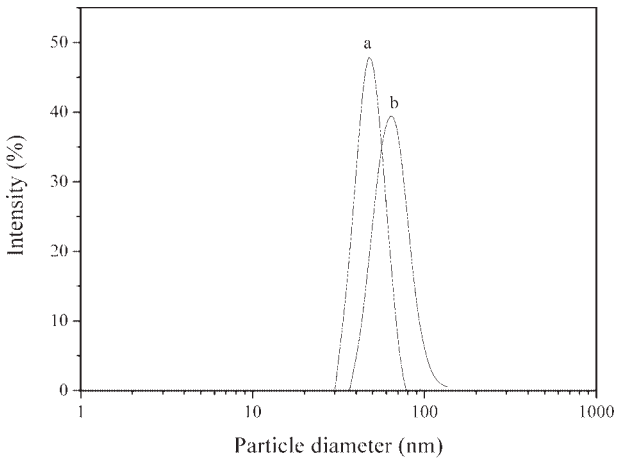

Figure 6 Particle diameter distributions of IPTT-Ca/PBA (a) and IPTT-Ca/ACR (b) latexes.

Particle diameter and morphology of IPTT-Ca/ACR composite latexes

The particle diameters and their distributions of the composite latexes (IPTT-Ca/ACR) in different synthetic stages are shown in Figure 6. When the first growth-stage emulsion polymerization was completed, the average particle size of IPTT-Ca/PBA (core layer) was about 49 nm, which was larger than the mean size of nano-$CaCO_3$ particles (25 nm). This indicated that the PBA had encapsulated on the surface of IPTT-Ca particles. The particle size of IPTT-Ca/ACR latex increased to 66 nm at the end of the emulsion polymerization. The polydispersities of their distribution of two synthetic stages were both less than 0.2. This showed that BA monomer and surfactants could be adsorbed onto the surface of IPTT-Ca, and surfactants acted as micelles to ensure the polymerization took place around the IPTT-Ca. The morphology of IPTT-Ca/ACR composite latex is observed by TEM, as shown in Figure 7. It could be seen that the particles consisted of a dark core, which was calcium carbonate, and a brighter shell, which was the polymer. The image indicated that the particles of nano-$CaCO_3$ treated with the titanate coupling agent (IPTT) were mainly separated and enwrapped by the polyacrylics.

Blending of IPTT-Ca/ACR particles with PVC resin

Distribution of IPTT-Ca/ACR particles in the PVC matrix

It is well known that the dispersion of filler in the polymer matrix can have a significant effect on the mechanical properties of the composites, especially when the filler size of nano-$CaCO_3$ decreases to nanometer scale. Figure 8 shows the TEM image of the IPTT-Ca/ACR/PVC blends. The dark nano-composite particles can be clearly observed in a light

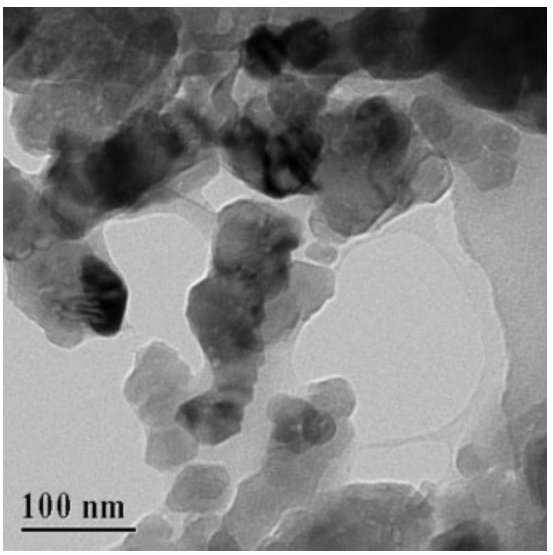

Figure 7 TEM image of IPTT-Ca/ACR composite latex.

background of PVC matrix. Most of IPTT-Ca/ACR particles were dispersed as primary particles with an average size of 60–70 nm, whereas very few were aggregated. This was due to the coated ACR polymer on the surface of IPTT-Ca particles, and a good dispersion of nano-inorganic particles in the matrix was achieved.

Mechanical properties of IPTT-Ca/ACR/PVC blends

The effects of IPTT-Ca/ACR particles on the Charpy notched impact strength of blends with PVC at different measuring conditions are shown in Figure 9. It can be seen from the curves that the notched impact strength of blends was higher than that of the pure PVC (6.68 kJ/m^2 at 23°C, and 3.05 kJ/m^2 at −20°C). This is because the titanate coupling agent

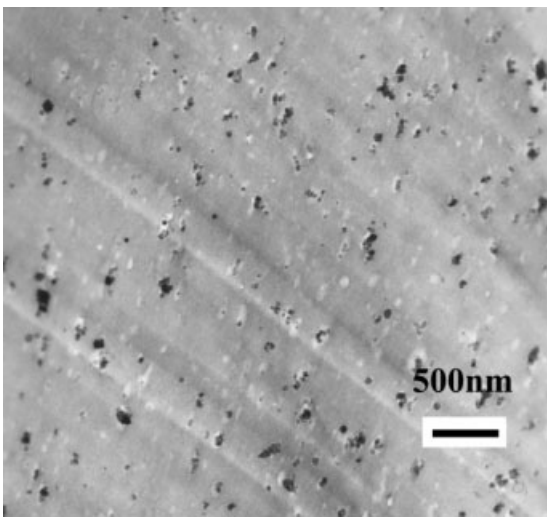

Figure 8 TEM image of IPTT-Ca/ACR/PVC blend (weight ratio of IPTT-Ca/ACR to PVC: 8/100).

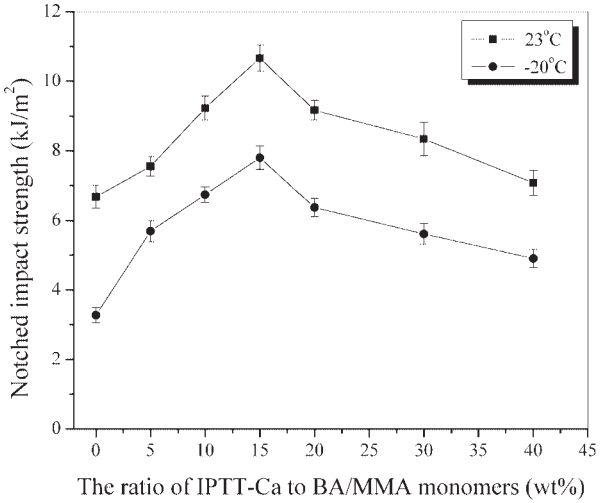

Figure 9 Curves of the notched impact strength of IPTT-Ca/ACR/PVC blends versus weight ratio of IPTT-Ca to BA/MMA monomers (weight ratio of BA to MMA: 6/4).

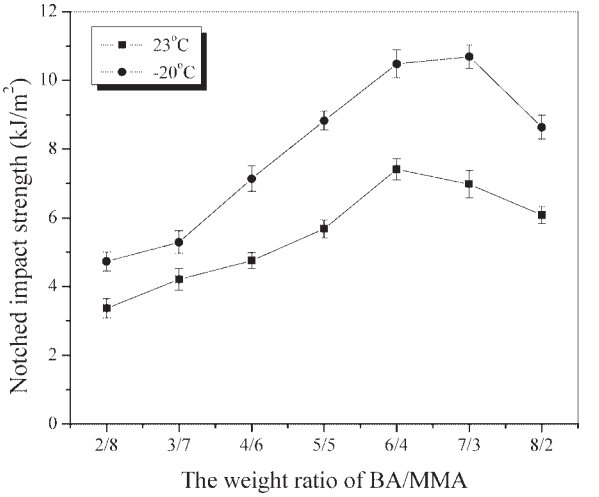

Figure 11 Curves of the notched impact strength of IPTT-Ca/ACR/PVC blends versus weight ratio of BA to MMA monomer.

has unsaturated chemical groups, which can introduce double-bonds onto the surface of nano-$CaCO_3$ particles through the surface modified reaction. The double-bond structure would bond with BA monomer in the emulsion polymerization, which led to strong junction in the inorganic-organic interphases. This is responsible for subsequent encapsulation of BA and MMA monomers to form the complete core-shell structured composite particles. The nano-$CaCO_3$ particle and polyacrylic were cohered tightly through the "bridging" effect of the titanate coupling agent. The toughening synergism of nano inorganic particles and elastic polymer display effectively. In view of the nano-$CaCO_3$ particles treated by IPTT coupling agent, the elastic polymer combined with nano-$CaCO_3$ through chemical bonding, so the interphase tension between nano-inorganic particle and the elastic was low, which made the toughing effectiveness of the composite particles on PVC matrix better. From Figure 9, we can see that there is an optimum value of the weight ratio of IPTT-Ca to monomers' content at 15%, which might mean that the toughening synergism of nano inorganic particles and elastic polymer was the strongest at this ratio.[12]

The tensile strength is an important character of polymer blends because it indicates the limit of final strength in most applications. The tensile strength of IPTT-Ca/ACR/PVC blends is almost independent of the ratio of IPTT-Ca to ACR monomers added, as shown in Figure 10. The smaller increase represents

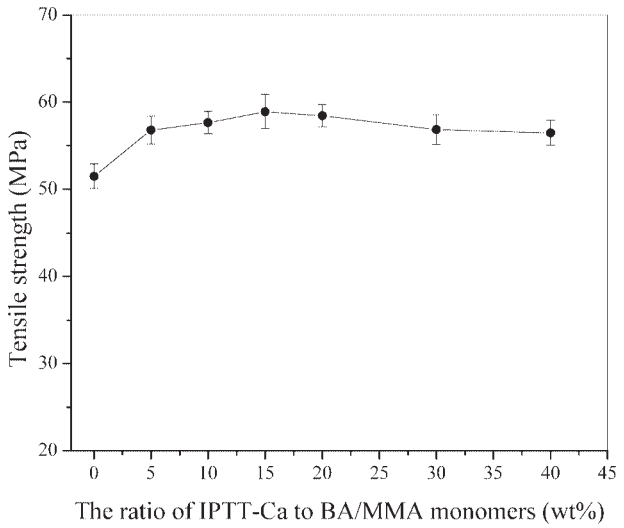

Figure 10 Curves of the tensile strength of IPTT-Ca/ACR/PVC blends versus weight ratio of IPTT-Ca to BA/MMA monomers (weight ratio of BA to MMA: 6/4).

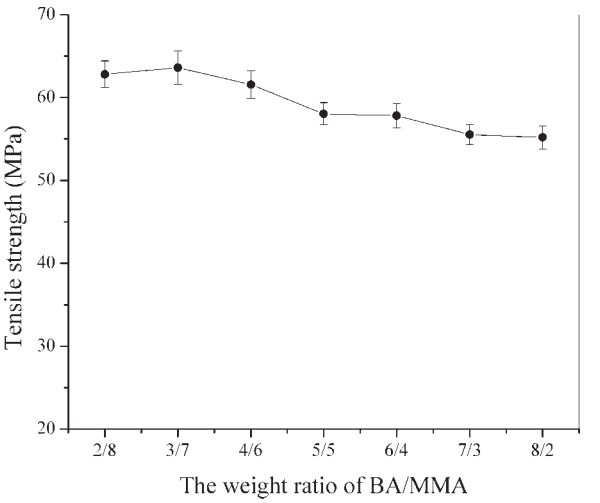

Figure 12 Curves of the tensile strength of IPTT-Ca/ACR/PVC blends versus weight ratio of BA to MMA monomer.

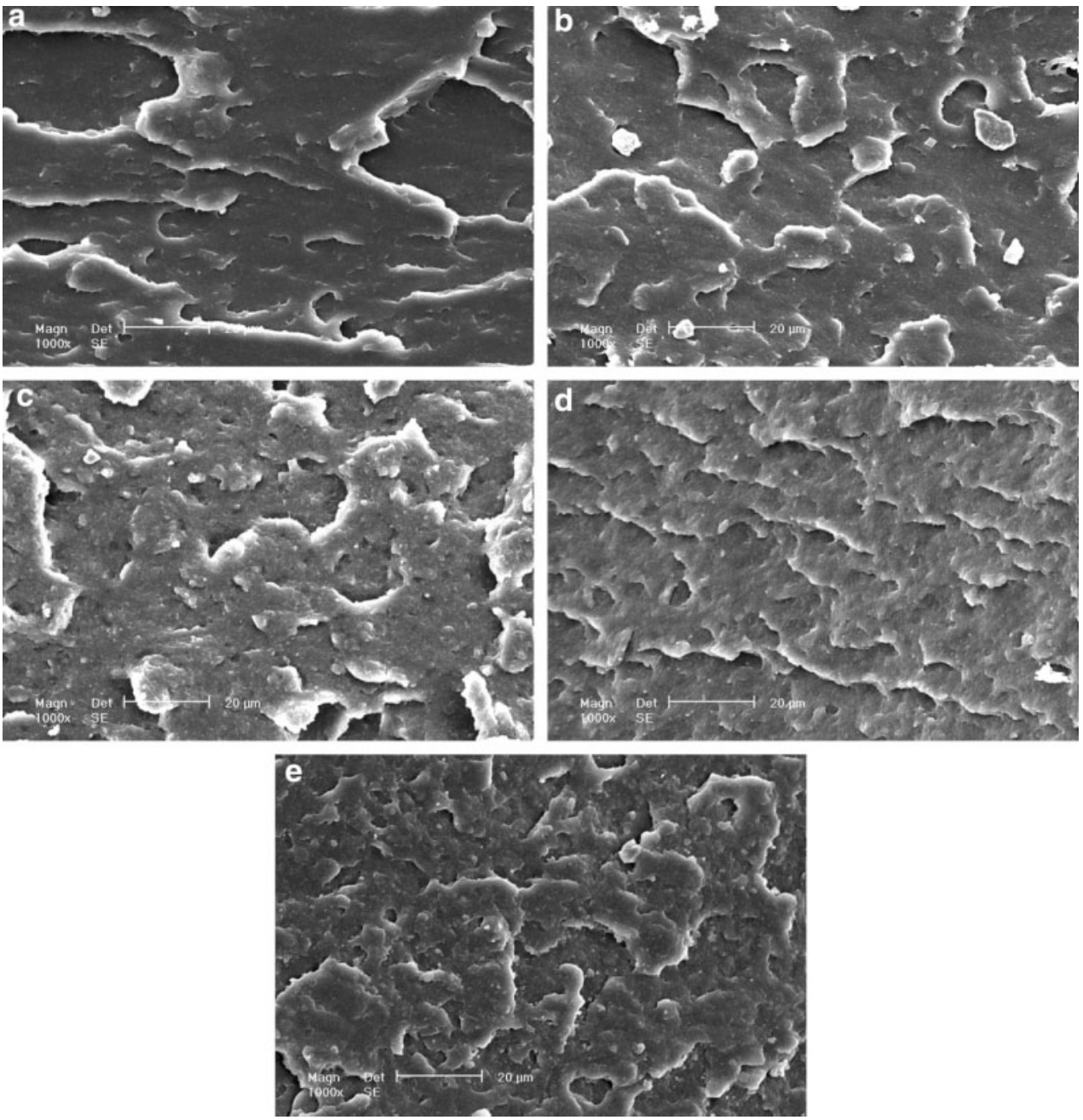

Figure 13 SEM microphotographs of the fractured surfaces of PVC blends with different composite structures, the weight ratio of the composite particle to PVC: 8/100, pure PVC (a), nano-$CaCO_3$/PVC (b), IPTT-Ca/PVC (c), IPTT-Ca/PBA/PVC (d), and IPTT-Ca/ACR/PVC (e) blends.

the existence of an interface region by which two phases are bonded strongly because the tensile strength is strongly dependent on the interface structure of the blends. Strong interactions resulted in good adhesion and efficient stress transfer from the continuous to the dispersed nano-$CaCO_3$ phase in the blends, as the stress had to transfer across the interface to avoid the fracture. Therefore, an improved toughness–stiffness balance can be obtained in IPTT-Ca/ACR/PVC blends by the introduction of IPTT coupling agent onto the surface of nano-$CaCO_3$.

The relations of the weight ratio of BA to MMA with the mechanical properties of the blends are shown in Figures 11 and 12. Figure 11 presents the notched impact strength of IPTT-Ca/ACR/PVC blends with different weight ratios of BA/MMA at room temperature (23°C) and low temperature (−20°C). When the ratio of IPTT-Ca/ACR polymer was fixed at 15 wt %, the notched impact strength of

blends increased with increasing the ratio of BA/MMA initially and then decreased when the ratio of BA/MMA was above 6/4. This is because the outermost shell, PMMA, acts to enhance the compatibility between PVC and IPTT-Ca/ACR composite particles. PMMA (the shell layer), having a solubility parameter very close to that of PVC (the matrix), is expected to have very good compatibility with PVC.[37] If the thickness of the outermost shell (PMMA) is suitable for the latex particles, The action of the IPTT-Ca/ACR composite particles would cause toughening of the PVC matrix by initiating crazes and shear bands.[1] Therefore, the ductility of blends became better with the increase of the BA content. However, when the ratio of BA/MMA reached to 7/3, the latex particles of IPTT-Ca/PBA could not be encapsulated by PMMA monomer completely, and uniform nanocomposite particles with core-shell structure could not be obtained after demulsification. This led to weakening of the compatibility between IPTT-Ca/ACR composite particle and PVC matrix. To get a good toughening modification, the weight ratio of BA/MMA was chosen as 6/4. The tensile property of blends appears to have a declining tendency with the increase of the weight ratio of BA/MMA, as shown in Figure 12. The interaction between PMMA and PVC is very strong, and their interfacial combination is also better, which can pass the internal stress. Meanwhile, with the increase of content of PBA elastic phase, the strengthening effect of nano-$CaCO_3$ particles on PVC matrix decreased significantly.

SEM microphotographs of fractured surface of the blends

Intuitively, it is believed that the features of the filler–matrix interfacial layer are responsible to a great extent for the morphologies of the fractured surface of PVC blends. Figure 13 shows SEM microphotographs of the impact-fractured surfaces of pure PVC (a), PVC/nano-$CaCO_3$ (b), PVC/IPTT-Ca (c), PVC/IPTT-Ca/PBA (d), and PVC/IPTT-Ca/ACR (e) blends. For the pure PVC, it can be seen from Figure 13(a) that there are many cavities leading to brittle failure. When untreated nano-$CaCO_3$ is added to PVC, small aggregates of nano-$CaCO_3$ particles can be observed in Figure 13(b). After the nano-$CaCO_3$ particles are treated with IPTT coupling agent, no visible particle agglomerates are observed, as shown in Figure 13(c). Well-dispersed particles appear distinguishable from the PVC matrix. As PBA polymers were encapsulated on the surfaces of the nano-$CaCO_3$ particles, the fractured surface of IPTT-Ca/PBA/PVC blend reveals some ductile deformation, shown in Figure 13(d). With high molecular mobility, PBA might act as a bumper interlayer around the fillers. It absorbed the impact energy and prevented the initiation of cracks. PBA is a rubber-like substance, and it is difficult for the IPTT-Ca/PBA composite particles to disperse in the PVC matrix uniformly. For the IPTT-Ca/ACR composite particles, the PVC matrices are highly deformed and drawn around the particles, as in Figure 13(e), because titanate coupling agent (IPTT) is grafted on the surface of calcium carbonate and PMMA shell is encapsulated on the surface of the IPTT-Ca/PBA latex particles.[38,39] PVC is compatible with PVC according to their close solubility parameters.[37] This led to increasing the interaction between the nano-$CaCO_3$ particles and PVC matrix, thus enhancing their dispersion in the PVC matrix and improving the tensile strength and impact strength for the large energy absorption of the blends.

CONCLUSIONS

The morphology and the grafting ratio of the treated nano-$CaCO_3$ with IPTT were affected by the weight ratio of IPTT to nano-$CaCO_3$. A high grafting ratio could be reached with proper reaction conditions. The synthesized IPTT-Ca/ACR core-shell particles were used to toughen the PVC matrix. The IPTT-Ca/ACR/PVC blends had a significant toughening effect because of the good dispersion and good adhesive interface between $CaCO_3$ and ACR in PVC matrix. The weight ratio of IPTT-Ca to BA/MMA monomers and the weight ratio of BA to MMA in the formation of ACR polymer influenced the mechanical properties of IPTT-Ca/ACR/PVC blends. The fractured surfaces of the blends exhibited significant ductile deformation of the PVC matrix, which was consistent with the impact properties of the blends.

The authors thank Prof. Peter A. Lovell, University of Manchester, UK, for many helpful discussions and the reviewers for their valuable comments on this article.

References

1. Wu, P. X.; Zhang, L. C. Polymer Blending Modification; China Light Industry Press: Beijing, China, 1996.
2. Knight, G. W. Polymer Toughening; Marcel Dekker: New York, 1996.
3. Pukanszky, B. Polypropylene: Structure, Blends and Composites; Chapman & Hall: London, 1995.
4. Peňa, J. R.; Hidalgo, M.; Mijangos, C. J Appl Polym Sci 2000, 75, 1303.
5. Berard, M. T.; Williams, S. M. J Vinyl Additive Tech 1996, 2, 117.
6. Takaki, A.; Yasui, H.; Narisawa, I. Polym Eng Sci 1997, 37, 105.
7. Li, K. C.; Tang, K. C.; Lee, J. S.; Chao, C. L.; Chang, R. K. J Vinyl Additive Tech 1997, 3, 17.

8. Zhang, L. C.; Pan, M. W.; Zhang, J. J Appl Polym Sci 2004, 91, 1168.
9. Caneba, G. T.; Kandiraju, S. Adv Polym Tech 1990, 10, 237.
10. Chakrabarti, R.; Das, M.; Chakraborty, D. J Appl Polym Sci 2004, 93, 2721.
11. Avella, M.; Errico, M. E.; Martelli, S. Appl Organometal Chem 2001, 15, 435.
12. Wu, D. Z.; Wang, X. D.; Song, Y. Z.; Jin, R. G. J Appl Polym Sci 2004, 92, 2714.
13. Zhang, K.; Chen, H. T.; Chen, X.; Chen, Z. M.; Cui, Z. C.; Yang, B. Macromol Mater Eng 2003, 288, 380.
14. Espiard, P.; Guyot, A. Polymer 1995, 36, 4391.
15. Chen, J. D.; Carrot, C.; Chalamet, Y.; Majeste, J. C.; Taha, M. J Appl Polym Sci 2003, 88, 1376.
16. Xia, H. S.; Zhang, C. H.; Wang, Q. J Appl Polym Sci 2001, 80, 1130.
17. Wang, Q.; Xia, H. S.; Zhang, C. H. J Appl Polym Sci 2001, 80, 1478.
18. Xu, G. C.; Li, A. Y.; Zhang, L. D.; Wu, G. S.; Yuan, X. Y.; Xie, T. J Appl Polym Sci 2003, 90, 837.
19. Luna-Xavier, J. L.; Bourgeat-Lami, E.; Guyot, A. Colloid Polym Sci 2001, 279, 947.
20. Luna-Xavier, J. L.; Guyot, A.; Bourgeat-Lami, E. J Colloid Interface Sci 2002, 250, 82.
21. Bourgeat-Lami, E.; Lang, J. J Colloid Interface Sci 1998, 197, 293.
22. Bourgeat-Lami, E.; Lang, J. J Colloid Interface Sci 1999, 210, 281.
23. Rong, M. Z.; Ji, Q. L.; Zhang, M. Q.; Friedrich, K. Eur Polym J 2002, 38, 1573.
24. Erdem, B.; Sudol, E. D.; Dimonie, V. L.; El-Aasser, M. S. J Polym Sci Part A: Polym Chem 2000, 38, 4419.
25. Erdem, B.; Sudol, E. D.; Dimonie, V. L.; El-Aasser, M. S. J Polym Sci Part A: Polym Chem 2000, 38, 4431.
26. Xu, W. B.; Liang, G. D.; Wang, W.; Tang, S. P.; He, P. S.; Pan, W. P. J Appl Polym Sci 2003, 88, 3225.
27. Xu, W. B.; Bao, S. P.; He, P. S. J Appl Polym Sci 2002, 84, 842.
28. Liu, G. D.; Zhang, L. C.; Qu, X. W.; Wang, B. T.; Zhang, Y. J Appl Polym Sci 2003, 90, 3690.
29. Kovačević, V.; Leskovac, M.; Lučićblagojević, S. J Adhes Sci Tech 2002, 16, 1915.
30. Domka, L. Colloid Polym Sci 1993, 271, 1091.
31. Tamai, Y.; Makuuchi, K.; Suzuki, M. J Phys Chem 1967, 71, 4176.
32. Henry, P.; Julian, B. J Phys Chem 1964, 68, 1586.
33. Zhu, Y.; Zhao, Z. G. The Base of Interfacial Chemistry; China Light Industry Press: Beijing, China, 1996.
34. Solomn, D. H. Chemistry of Pigement and Fillers; John Wiley: New York, 1983.
35. Yang, L.; Hong, J.; Wang, J.; Pilliar, M. R.; Santerre, P. J. Biomaterials 2005, 26, 5951.
36. Sheng, Y.; Zhou, B.; Zhao, J. Z.; Tao, N. N.; Yu, K. F.; Tian, Y. M.; Wang, Z. C. J Colloid Interface Sci 2004, 272, 326.
37. Chakrabarti, R.; Chakraborty, D. J Appl Polym Sci 2005, 97, 1725.
38. Wu, C. L.; Zhang, M. Q.; Rong, M. Z.; Friedrich, K. Compos Sci Technol 2005, 65, 635.
39. Wu, G. F.; Zhao, J. F.; Shi, H. T.; Zhang, H. X. Eur Polym J 2004, 40, 2451.